Title

High Asymmetric Longitudinal Field Ion Mobility Spectrometry Device for Low Power Mobile Chemical Separation and Detection

Journal

Analytical Chemistry, 91(9)

ISSN

0003-2700

Authors

Zrodnikov, Yuriy

Rajapakse, Maneeshin Y

Peirano, Daniel J

et al.

Publication Date

2019-05-07

DOI

10.1021/acs.analchem.8b05577

Peer reviewed

HHS Public Access

Author manuscript

Anal Chem. Author manuscript; available in PMC 2022 December 28.

Published in final edited form as:

Anal Chem. 2019 May 07; 91(9): 5523–5529. doi:10.1021/acs.analchem.8b05577.

High Asymmetric Longitudinal Field Ion Mobility Spectrometry (HALF-IMS) device for low power mobile chemical separation and detection

Yuriy Zrodnikov[1,§], **Maneeshin Y. Rajapakse**[1], **Daniel J. Peirano**[1,†], **Alexander A. Aksenov**[1,‡], **Nicholas J. Kenyon**[2,3,4], **Cristina E. Davis**[1,*]

[1]Department of Mechanical and Aerospace Engineering, University of California Davis, Davis, CA 95616, USA.

[2]Department of Internal Medicine, 4150 V Street, Suite 3400, University of California, Davis, Sacramento, CA 95817, USA.

[3]Center for Comparative Respiratory Biology and Medicine, University of California, Davis, CA 95616, USA.

[4]VA Northern California Health Care System, 10535 Hospital Way, Mather, CA 95655, USA.

Abstract

We have developed a novel chemical sensing technique termed High Asymmetric Longitudinal Field Ion Mobility Spectrometry (HALF-IMS), which allows separation of ions based on mobility differences in high and low electric fields. Our device is microfabricated, has a miniature format, and uses exceptionally low power due to the lack of RF separation fields normally associated with ion mobility spectrometry (IMS) or differential mobility spectrometry (DMS). It operates at room temperature and atmospheric pressure. This HALF-IMS chip contains a microscale drift cell where spatially-varying electric field regions of high and low strengths are generated by direct current (DC) applied to the electrodes that are physically placed to cause ionic separation as the ionized chemical flows along the drift cell. Power and complexity is reduced at the chip- and system-level by reducing the voltage magnitude and using DC-powered electronics. A testing platform utilizing an ultraviolet (UV) photoionization source was used with custom electronic circuit boards to interface with the chip and provide data inputs and outputs. Precise control of the electrode voltages allowed filtering of the passage of the ion of interest through the drift cell and ionic current was measured at the detector. The device was tested by scanning of electrode voltages and obtaining ion peaks for methyl salicylate, naphthalene, benzene and 2-butanone. The

[*]**Corresponding Author** (CED) cedavis@ucdavis.edu.
[§]presently at Intel Corporation, Inc.
[†]presently at Google, Inc.
[‡]presently at University of California, San Diego

The authors declare that a patent application has been submitted on part of the work presented in this paper.

DEVICE DESIGN AND CODE INFORMATION

The PCB design specifications and microcontroller code and for the HALF-IMS device are available on GitHub. Please refer to Professor Cristina Davis' webpage for more information. The software code and PCB design specifications are available for academic/nonprofit research and personal use only. Commercial licensing may be available. All code and PCB designs are ©The Regents of the University of California, Davis campus, all other rights reserved. Future published scientific manuscripts or reports using this software and/or hardware designs must cite this original publication (DOI: xxxx-xxx-xxxx-x).

current experimental setup was capable of detecting as low as ~ 80 ppb of methyl salicylate and naphthalene. The use of benzene as a dopant with 2-butanone allowed to see two ion peaks, corresponding to benzene and 2-butanone.

INTRODUCTION

There are an increasing number of public health and safety threats that require improved chemical detection technologies that are fast and precise at trace levels, including explosives detection, alerting for drug trafficking activity, and environmental pollutant monitoring. Large benchtop chemical detection systems, mass spectrometry, gas and liquid chromatography (GC and LC), ion mobility spectrometry (IMS), and differential mobility spectrometry (DMS) are capable of achieving these requirements[1]. However, there are few feasible detectors for ultra-low power portable field applications with real-time sampling and trace detection in austere environments. The limitations of aforementioned techniques preventing their direct application include large size, high power and supporting hardware requirements, as well as lengthy analysis time.

Microelectromechanical systems (MEMS) chemical sensors can be light-weight, portable and inexpensive with high-scale manufactured. Currently-developed MEMS sensors include electronic nose (E-Nose), metal oxide sensors and high field asymmetric ion mobility spectrometry sensors [2–4]. Metal oxide sensors (MOS) can only be tuned to one or few chemicals of interest and are not practical for analyzing complex gas phase mixtures and ultra-trace limits of detection. E-Nose technologies take many forms and can be used for complex mixtures, but many drift significantly over time and with varying operating conditions. High field asymmetric ion mobility spectrometry (FAIMS) sensors have good reported performance with both single chemicals and mixtures, but their portable uses are limited by high voltage and power consumption requirements [5–6]. Ion mobility-based detection systems (IMS, DMS and FAIMS) can be made into small-footprint detectors for significantly less cost compared to GC, LC and MS techniques leading to their use in agriculture, food safety, healthcare and even space explorations [6–10]. However, power requirements have still prevented these valuable sensors from being included into massively-parallel networks of miniature chemical sensors in an “internet-of-things” approach to detect chemicals across widely varying space and time profiles (e.g. a multitude of sensor nodes spread across an entire city infrastructure).

Even the smallest IMS cells are larger in size compared to any DMS cells and those require high DC voltages to generate electric fields and ion shutters to gate ions for the ion separation[11–13]. Ion separation in DMS happens between two closely spaced planar electrodes. The ions are driven by a carrier gas from an ionization source to the detectors, and ions undergo oscillations due to the strong electric field of ~ 30 kV which is established between the electrodes by an asymmetric waveform having MHz-frequency. The ion velocity (v) perpendicular to each electrode can be denoted by the equation (1), where K(E) is the field dependent ion mobility and E is time dependent electric field strength [3].

$$v = K(E)\ x\ E \quad (1)$$

Ion trajectories are unique for each different chemical ion species, as they are “steered” towards upper or lower electrode plane. The ions with total transverse displacements less than the gap between the two electrodes will pass through and their charge will be measured at the detector. Other ions having a net drift greater than the gap between electrodes will neutralize by colliding with electrode surfaces and will be purged by the carrier gas. Desired ions can be passed between the two electrodes by directing DC voltage, which is known as a compensation voltage (CV). This architecture enables this device to function as an ion filter based on the differential mobility spectrum. Unlike IMS, DMS can collect both negative and positive ion spectra simultaneously using two independent Faraday detectors at the end of each filter electrodes. When both CV and RF voltages are scanned a detailed 3-dimentional dispersion plot of detected ions can be obtained.

Both IMS and DMS devices have been miniaturized to portable versions and those include the IMS Chemical Agent Monitor (Smiths Detection- Watford Ltd, Watford, UK), Ion Scan™ (Smiths Detection, Edgewood, MD) and the MobileTRACE® (Rapiscan Systems, Torrance, CA)[1, 3]. MEMS manufacturing allows further miniaturization of these devices, and a DMS device was successfully demonstrated[3]. However, these sensors inherited previous generation designs, such as electronics and physical layouts that hinder the advantages gained by miniaturization. High voltages with power-demanding complex circuitry designs are required for RF voltage generation in DMS, and physical ion shutters and difficult miniaturization of cylindrical drift tubes in IMS are major obstacles.

We have developed an entirely new concept for a MEMS-based sensor that allows for the performance benefits of ion mobility separation of chemicals, but without the power consumptions demanded by the RF waveform circuitry or physical ion shutters. This is the first report of this HALF-IMS design, operation principles, fabrication process and demonstration of chemical separation and detection.

EXPERIMENTAL

Design and Operating Principle.

The HALF-IMS was developed to address the fore-mentioned shortcomings, especially relating to power requirements due to the RF waveform generator. The device layout (Figure 1) is similar to FAIMS or DMS at the system level, consisting of: an ionization source, parallel-plate drift tube, and pair of positive and negative ion detectors. Unlike FAIMS, our HALF-IMS creates spatially-varying static electric fields along the drift tube region using constant DC voltages. Alternating short and long electrodes paired sets are longitudinally arrayed down the drift cell (Figure 1a). A lower magnitude DC voltage difference is applied between upper and lower long electrodes to direct the electric field (E-field) towards the upper electrode, while a higher magnitude DC voltage is applied between the upper and lower short electrode sets to create higher-strength E-field directed toward the lower electrode. To separate ions, the ratio between the lower strength field across the longer electrode and the upper strength field across the lower electrode must

balance, while accounting for field-dependent ion mobility of the particular chemical ion species at higher strength fields. A regime, which yields zero net vertical ion drift along the drift tube length, will allow chemicals to be detected by the positive- and negative-biased detector plates.

Computational Calculations.

COMSOL Multiphysics (version 5.3a) and AC/DC modules (version 4.2) were used to simulate electric field distributions along the HALF-IMS drift tube. The input parameters and boundary conditions are shown (Figure 1b) with a long electrode length (L_L), short electrode length (L_S), electrode thickness (t), gap size (g). Spacing between electrodes was 10 μm and the tested gap size was 50 μm, due to on-site microfabrication capabilities. The geometry allowed for electric field strengths of 12 kV/cm vertically between short electrode pairs with V_s = 30 V. Computational models showed local E-field zones surrounding electrode edges to be multidirectional which would disrupt drift path of ions entering these regions (Figure 1c). As the experimentation of Townsend breakdown showed, at 10 μm distance between electrodes, breakdown is not expected to occur below 50 kV/cm.

With long and short electrode lengths of 50 μm and 10 μm, the drift tube consisted of 220 electrode sets in total. In earlier DMS/FAIMS devices with MHz-frequency, drift tube ion residence times on the order of a few milli seconds and an ion typically underwent approximately 100–1000 RF cycles. The HALF-IMS reached comparable parameters using steady-state DC voltages to generate the E-fields.

Fabrication Process Flow.

The HALF-IMS fabrication process is shown (Figure 2) and was carried out in a class-100 cleanroom facility (Center for Nano and Micro Manufacturing (CNM2), UC Davis). The substrate was 100 mm round, 700 μm thick Borosilicate glass wafers (Borofloat® 33; Schott North America, Inc., Louisville, KY). Lithography was used to pattern the electrodes, followed by electron beam deposition of conductive Cr/Au thin film layers having thicknesses of 15/40 nm, and then a lift-off process to remove the photoresist and sacrificial layers. Dicing of the wafer with uniform spacing created chip halves, which were aligned and thermally bonded to prepare for testing (Figure 3).

Experimental Setup.

The HALF-IMS chip was assembled into a testing platform consisting of electronics and chemical/gas flow control (Figure 4). The chip had a total length of 36 mm, a drift cell length of 17.75 mm, and had 220 long electrodes with 50 μm width and 220 short electrodes with 10 μm width along the drift cell region.

Purified air (Air Gas, Radnor, PA) (water content ~ 2 ppm) was used as the carrier gas for all flow settings. The sample gas flow was kept constant at 20 mL/min and a vapor generator was used to control concentrations within carrier gas having constant flow of 100 mL/min. Volatile samples were prepared in the vapor generator by adding glass diffusion tubes in line. These diffusion tubes were weighed over several days at constant flow and room temperature to obtain the weight loss of a sample over that duration, and the

concentrations were calculated. Carrier gas flow was driven into the system through a 3-way front flange that facilitates a sealed interface between the Ultraviolet (UV) bulb ionization source (Kr, 10.6 eV, Model 510106, Andrews Glass Company, Vineland, NJ) and the inlet of the HALF-IMS chip using a laser-cut 10×5×0.6 mm elastic gasket (PN: 86465K21, McMaster-Carr, Santa Fe Springs, CA). Concentrated sample gas exited through a 1 mm diameter hole on one of the HALF-IMS planes (Figure 4), as regulated by an attached mass flow controller (APEX, Model: AX-MC-500 SCCM-D/5M, Canton, GA) and vacuum pump (Model: MOA-P101-AA, GAST Manufacturing Inc., Benton Harbor, MI) with 10×5×0.6 mm elastic gaskets, Teflon tubing and Swagelok unions (Solon, OH) that provided a sealed connection to maintain a constant carrier gas flow. The dopant gas line (20 ml/min, 500 ppb) was only added for the detection of 2-butanone to the carrier gas stream before the sample gas inlet. The carrier gas flow was adjusted when the dopant was introduced to keep constant total flow at 100 ml/min. The testing components and sample tubing were kept at room temperature and thorough purging of carrier gas through the system was performed with measurements of background spectra between each new chemical measurement to ensure the drift cell was free of carry-over contamination.

Electrical spring-connectors (821–22-004–10-000101, Mill-Max, Oyster Bay, New York) connected the chip conductive traces to the controlling circuit boards. LabVIEW software and dedicated hardware (PXI 8101, PXI-6723, PXI-6281, National Instruments, Austin, TX) were used to output voltage at the HALF-IMS electrodes and measure current at the detectors, both with a rate of 1 kHz. For all experimentation, the ionization source was powered on and ionic current logged continuously. The HALF-IMS device was operated by controlling 4 voltages, with positive polarity voltage ($+V_l$) applied to upper plane long electrodes and negative polarity voltage ($-V_l$) applied to lower plane long electrodes; as well as $-V_s$ and $+V_s$ applied to upper and lower short electrodes, respectively. Several regimes were used for data collection (Figure S2), including a one-dimensional scan with V_L constant and V_s incremented continuously. The ions formed at the ionization source were carried by the carrier gas (Purified Air, Air gas, Radnor, PA) at a flow rate of 100 mL/min between the two parallel drift tube plates and detected by the two-faraday plates similar to past DMS devices. After sampling was finished, input and output data were aligned by timestamp and used for analysis. A moving 11-points average of was used to filter high frequency electronic noise from the data.

RESULTS AND DISCUSSION

Chemical Detection.

The HALF-IMS assembly was leak tested to verify carrier gas flow through the HALF-IMS chip. V_L voltage was set to 3 V (1.2 kV/cm) and V_S voltage was scanned from 0–30 V during all experiments and positive ion spectra were considered in this analysis. Background spectra were collected with the operation of the UV bulb and without any sample introduction to verify the initial conditions of the HALF-IMS device. The krypton lamp ionization energy (10.60 eV) is insufficient to ionize any carrier gas components (nitrogen, oxygen, carbon dioxide and moisture); as expected, purified air alone produced no ion peaks during these tests (data not shown). Methyl salicylate (IE = 7.65 eV), naphthalene

(IE = 8.14 eV), benzene (IE = 9.24 eV) and 2-butanone (IE = 9.52 eV) were selected based on the UV ionization energies for this study [14]. When the UV ionization energy of emitted photons is sufficient, chemical molecules can undergo ionization as shown by equation 2.

$$M + h\upsilon \rightarrow M^{+} + e^{-} \quad (2)$$

Sample ion peaks were obtained for methyl salicylate (Vs = 8.65 V), naphthalene (Vs = 8.80 V) and benzene (Vs = 9.00 V), and those spectra (concentrations were ~ 200 ppb for all the chemicals) are shown (Figure 5). However, 2-butanone alone did not produce any measurable ion peaks, previously observed by Nazarov *et al.* [15].

Benzene was introduced as a dopant to the system with the presence of 2-butanone and two ion peaks were obtained in positive mode HALF-IMS spectrum (Figure 5d). Possible product ions, in this type of experiment maybe identified as the UV ionized Benzene, $C_6H_6^+$ and the protonated butanone $(C_4H_8O)H^+$. Nazarov *et al* suggested two possible reaction mechanisms for the formation of protonated 2-butanone [15]. Both mechanisms go through a complex formation between protonated benzene and 2-butanone

The resulting two peaks in this HALF-IMS spectrum may be assigned as $C_6H_6^+$ (Peak 1, Vs_1 = 8.59 V) and the protonated butanone $(C_4H_8O)H^+$ (Peak 2, Vs_2 =10.36 V). Broad testing was limited mainly by the choice of benzene as a dopant that resulted in swelling of the silicone-based gasket, used to keep gastight seal between the 3-way flange and the inlet of the HALF-IMS chip [16]. The swollen gasket diminished flow through the chip within less than a minute of introducing benzene. The UV ionization source and room temperature (28 ^{o}C) operation of the HALF-IMS device and tubing limited the initial tests only to a handful of volatile chemicals.

The limited peak separation along the V_s scale during the single-chemical analysis (Figure 5a–c) may be due to the limited maximum effective field strength and the limited number of oscillations (equivalent to the total number of short and long electrode pairs) an ion under go in a HALF-IMS device compared to the DMS devices. Planar DMS separation increases with field strength and devices used fields as high as 30 kV/cm which is the upper limit for electrical breakdown between the upper and lower electrode in parallel. The maximum vertical field strength in the fabricated HALF-IMS chips was limited to 12 kV/cm to prevent electrical breakdown between adjacent sets of long and short electrodes. The variation of V_s value attributed to benzene peak (Figure 5c and 5d) may be impacted by a possible change of career gas flow during the analysis due to the swelling of the inlet gasket.

Chemical Sensitivity.

Methyl salicylate and naphthalene were used to obtain calibration curves. Samples were introduced into the system by a vapor generator as described in the Experimental Setup section to generate different concentrations and n=4 repetitive measurements were performed at each concentration. Concentrations were varied from 80–300 ppb and the results show that the device can detect as low as 80 ppb for both chemicals (Figure 6). Lower detection should be possible with advances in the detector electronics.

System Electronics.

The HALF-IMS features a low power drift tube having only static DC voltage with negligible current. Voltage amplifying circuitry was estimated to utilize less than 1 W of power. Detection circuitry was DC as well, powered using two 9 V batteries with estimated total power below 0.1 W. At the system level, the Krypton UV ionization bulb was powered with 1 W source. Testing was done using a benchtop 110 VAC pump (Model: MOA-P101-AA, GAST Manufacturing Inc., Benton Harbor, MI) vacuum mode by establishing the desired carrier gas flow.

CONCLUSIONS

We describe a new HALF-IMS device which uses a spatially-varying electric fields to separate ions longitudinally along a drift cell based on differences in ion mobility at high and low strength electric fields. Chips having a drift cell gap of 50 μm for sample flow were microfabricated and tested using a photoionization source. Methyl salicylate, naphthalene and benzene were detected by this HALF-IMS chip. Chemical separation was observed by introducing a dopant, benzene and detection of 2-butanone as two peaks in the same spectrum. Ion peaks for Methyl salicylate and Naphthalene were observed at the lowest tested level of ~ 80 ppb. A future HALF-IMS cell will include heated drift region and transfer lines, high-resolution electrodes, smaller dimension electrodes with a smaller gap size between plates that will allow increasing the electric fields between the electrodes to achieve better peak separation. Simultaneous scanning of both long and short electrodes is currently under consideration with the new HALF-IMS version to obtain 3-dimentional plots similar to DMS dispersion plots.

Supplementary Material

Refer to Web version on PubMed Central for supplementary material.

ACKNOWLEDGEMENTS

Partial support was provided by: NIH award U01 EB0220003-01 (CED, NJK); NSF award 1255915 (CED); The Hartwell Foundation (CED, NJK); NIH award UG3-OD023365 (CED, NJK); the NIH National Center for Advancing Translational Sciences (NCATS) through grant #UL1 TR000002 (CED, NJK); and NIH award 1P30ES023513-01A1 (CED, NJK). Student support was partially provided by the US Department of Veterans Affairs, Post-9/11 GI-Bill (DJP), and the NSF award 1343479 Veteran's Research Supplement (DJP). The authors would like to thank Danny Yeap for the assistance with data analysis. The contents of this manuscript are solely the responsibility of the authors and do not necessarily represent the official views of the funding agencies.

REFERENCES

1. Eiceman GA; Karpas Z; Hill HH, Ion Mobility Spectrometry, 3rd Edition. Ion Mobility Spectrometry, 3rd Edition 2014, 1–400.
2. Eiceman GA; Nazarov EG; Miller RA; Krylov EV; Zapata AM, Micro-machined planar field asymmetric ion mobility spectrometer as a gas chromatographic detector. Analyst 2002, 127 (4), 466–471. [PubMed: 12022642]
3. Miller RA; Eiceman GA; Nazarov EG; King AT, A novel micromachined high-field asymmetric waveform-ion mobility spectrometer. Sensor Actuat B-Chem 2000, 67 (3), 300–306.

4. Hichwa PT; Davis CE, Modern Application Potential of Miniature Chemical Sensors. In Sensors for Diagnostics and Monitoring, 1 ed.; Kevin Yallup LB, Ed. CRC Press, Taylor and Francis Group: Boca Raton, 2018; pp 283–302.
5. Krebs MD; Zapata AM; Nazarov EG; Miller RA; Costa IS; Sonenshein AL; Davis CE, Detection of biological and chemical agents using differential mobility spectrometry (DMS) technology. IEEE Sensors 2005, 5 (4), 696–703.
6. Aksenov AA; Pasamontes A; Peirano DJ; Zhao WX; Dandekar AM; Fiehn O; Ehsani R; Davis CE, Detection of Huanglongbing Disease Using Differential Mobility Spectrometry. Analytical Chemistry 2014, 86 (5), 2481–2488. [PubMed: 24484549]
7. Puton J; Namiesnik J, Ion mobility spectrometry: Current status and application for chemical warfare agents detection. Trac-Trend Anal Chem 2016, 85, 10–20.
8. Vautz W; Zimmermann D; Hartmann M; Baumbach JI; Nolte J; Jung J, Ion mobility spectrometry for food quality and safety. Food Addit Contam 2006, 23 (11), 1064–1073. [PubMed: 17071508]
9. Johnson PV; Beegle LW; Kim HI; Eiceman GA; Kanik I, Ion mobility spectrometry in space exploration. International Journal of Mass Spectrometry 2007, 262 (1–2), 1–15.
10. Chouinard CD; Wei MS; Beekman CR; Kemperman RHJ; Yost RA, Ion Mobility in Clinical Analysis: Current Progress and Future Perspectives. Clin Chem 2016, 62 (1), 124–133. [PubMed: 26585928]
11. André Ahrens SZ, A miniaturized drift tube ion mobility spectrometer for hand-held devices. In AMA Conferences – SENSOR and IRS2 2017, Exhibition Center in Nuremberg, Germany, 2017.
12. Sandia; National; Laboratory Miniature Ion Mobility Spectrometer. https://www.sandia.gov/mstc/_assets/documents/Fact_Sheets/sensors/2IMS.pdf (accessed Oct 24).
13. Xu J; Whitten WB; Ramsey JM, A MINIATURE ION MOBILITY SPECTROMETER. Int J Ion Mobil Spectrom 2002, 5 (2), 207–214.
14. NIST NIST, Gas phase ion energetics data. https://webbook.nist.gov/ (accessed Oct 21).
15. Nazarov EG; Miller RA; Eiceman GA; Stone JA, Miniature differential mobility spectrometry using atmospheric pressure photoionization. Anal Chem 2006, 78 (13), 4553–63. [PubMed: 16808465]
16. Characteristic properties of Silicone Rubber Compounds. https://www.shinetsusilicone-global.com/catalog/pdf/rubber_e.pdf (accessed Oct 21).

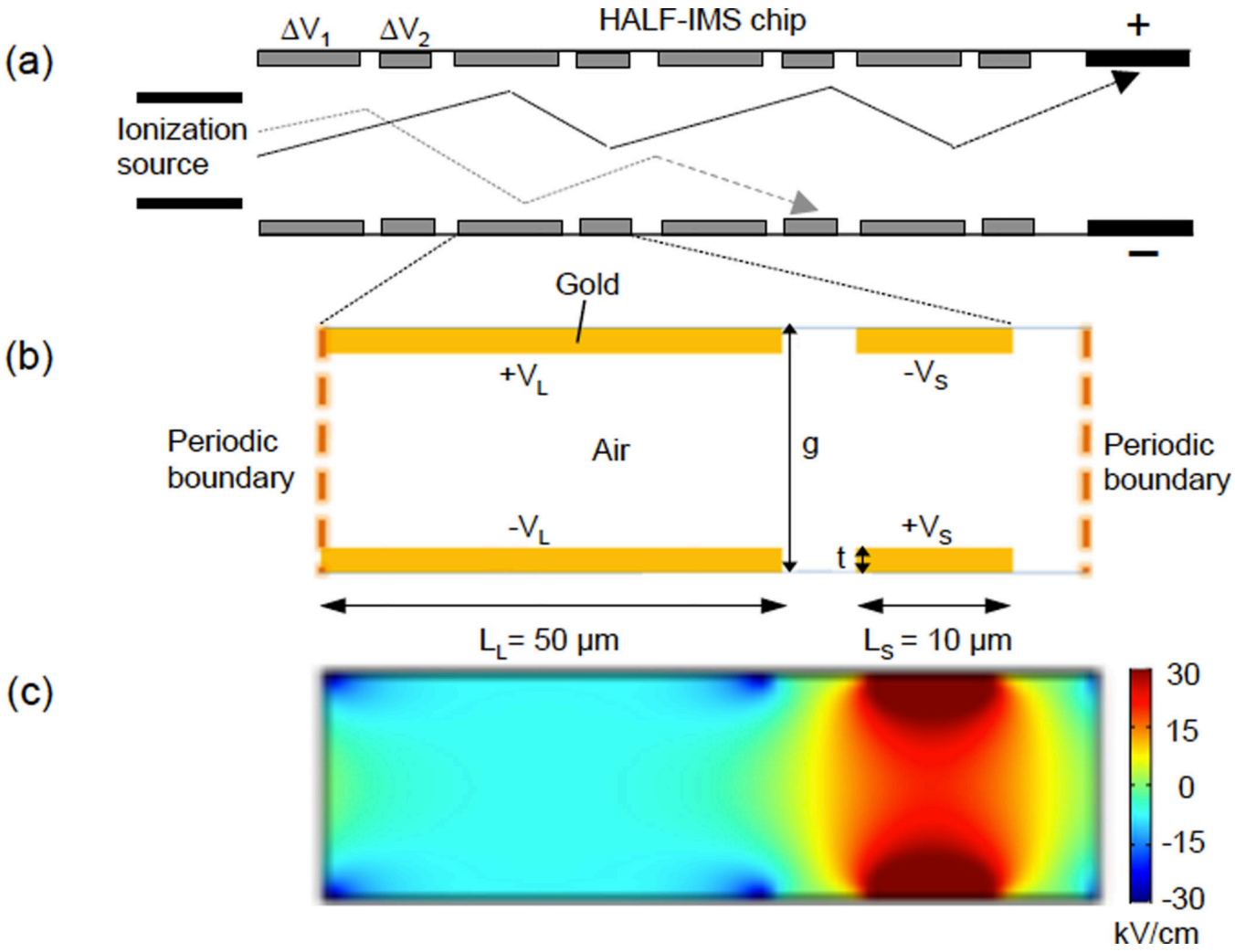

Figure 1:
HALF-IMS design with (a) layout of electrodes with ion motion; (b) key design parameters illustrated; and (c) computed electric field strengths within the drift cell.

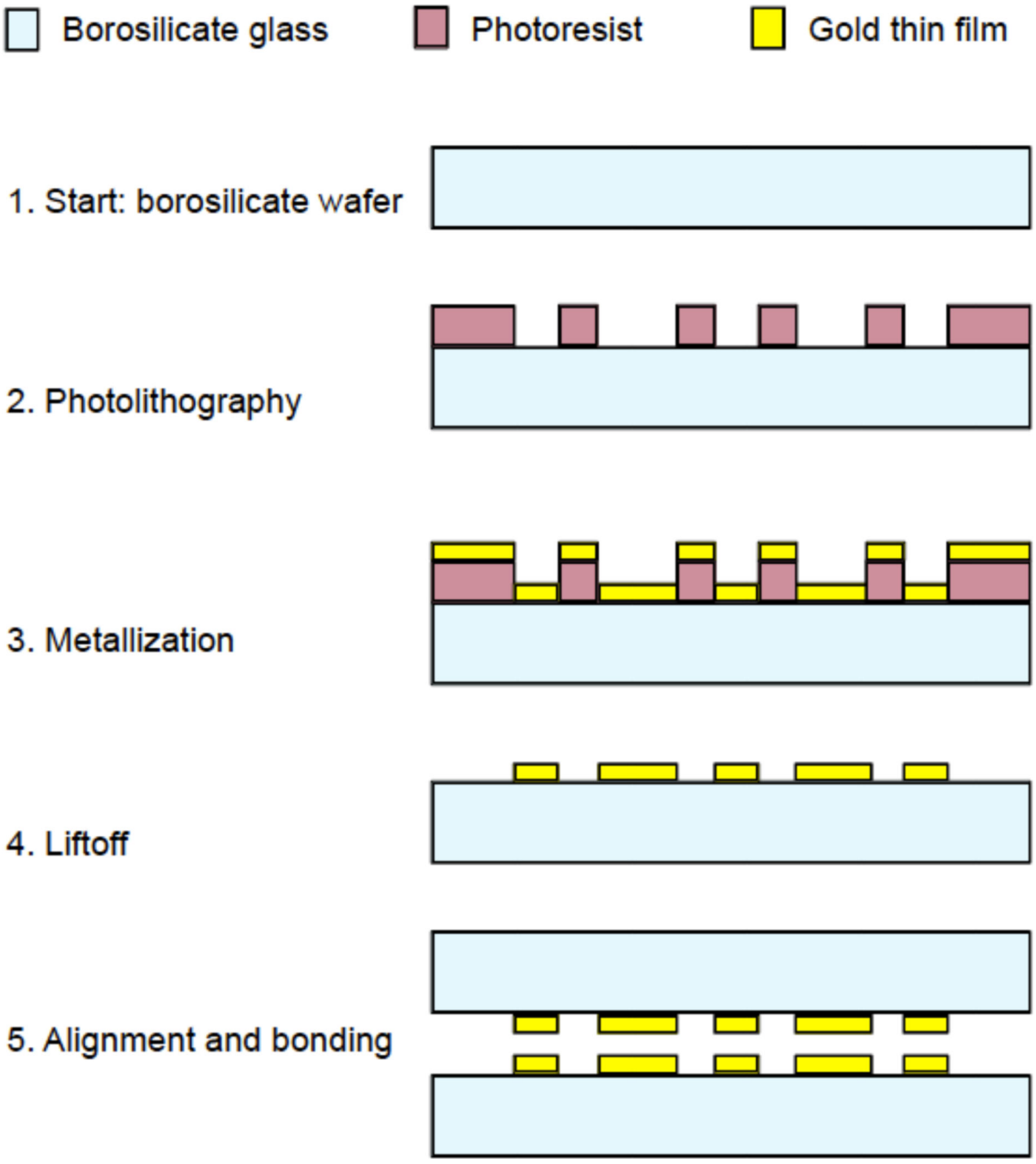

Figure 2:
HALF-IMS chip microfabrication process flow.

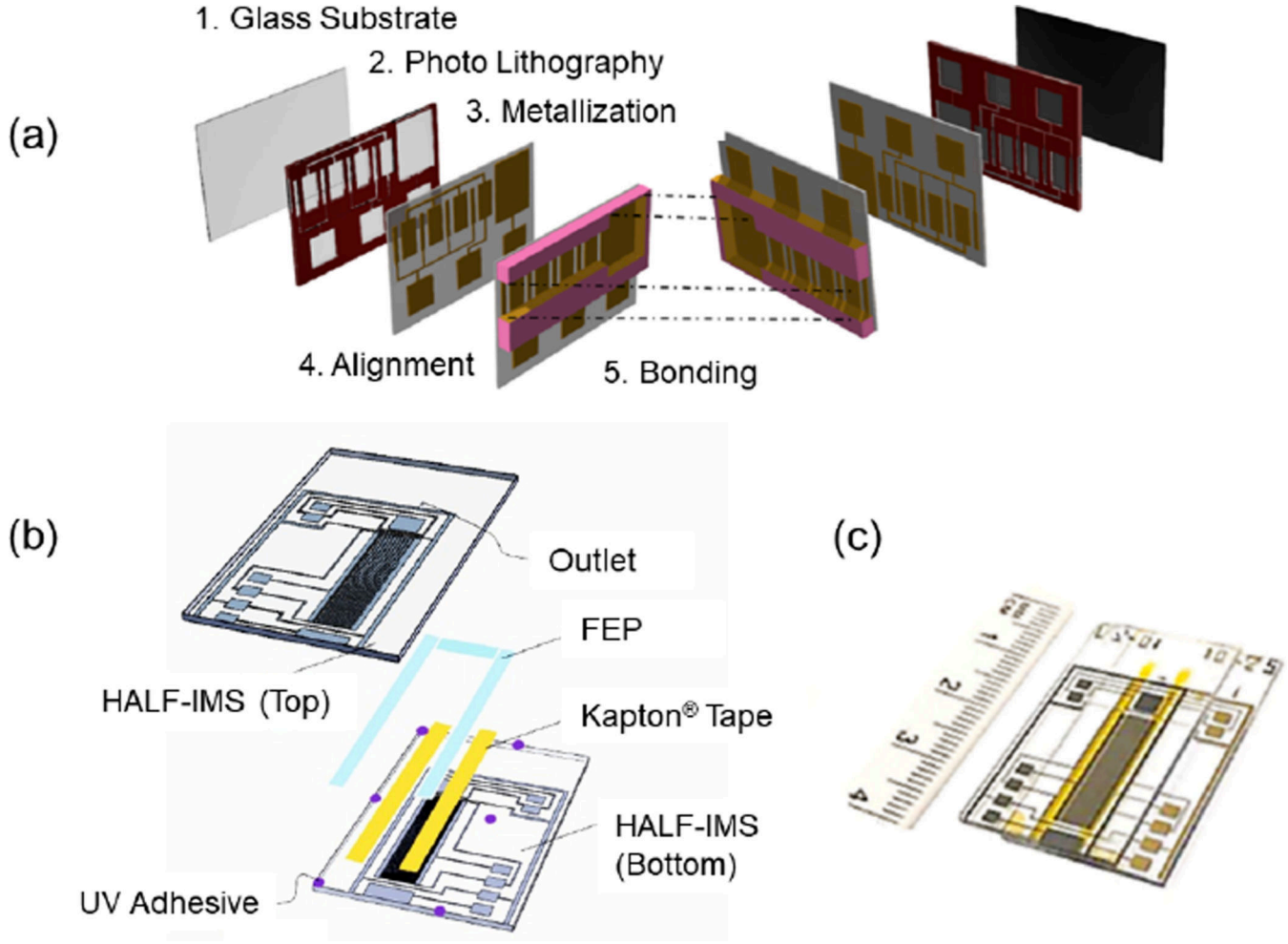

Figure 3:
HALF-IMS chip assembly (a) process flow, (b) alignment and bonding, and (c) final HALF-IMS chip.

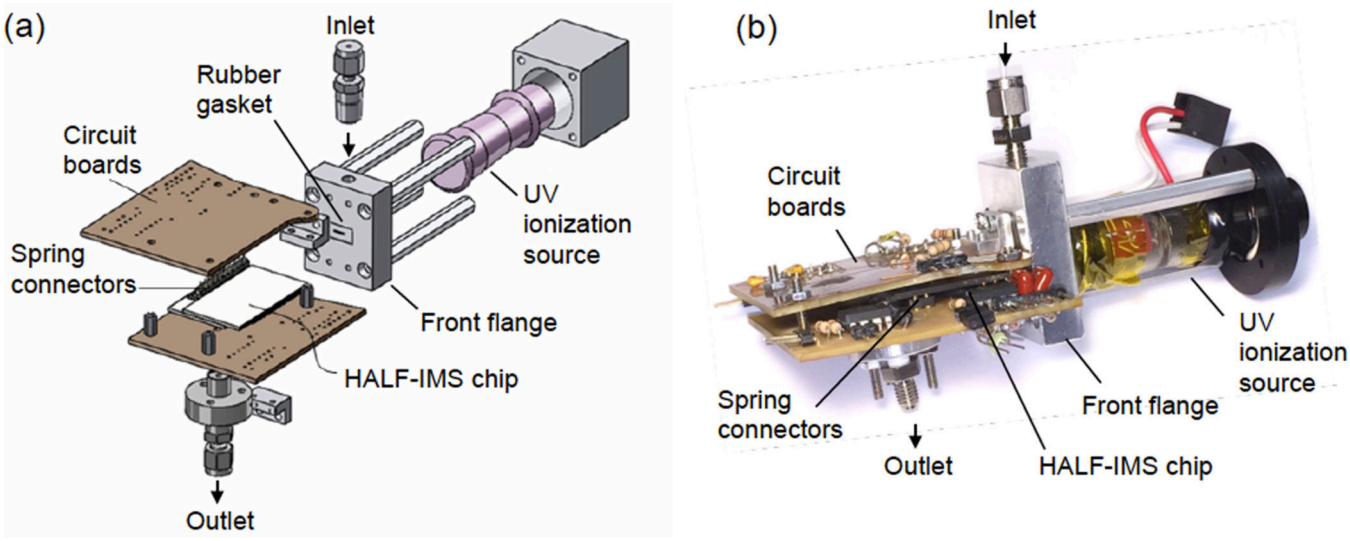

Figure 4:

HALF-IMS device assembly including (a) 3-dimensional drawing, and (b) image of the functional device

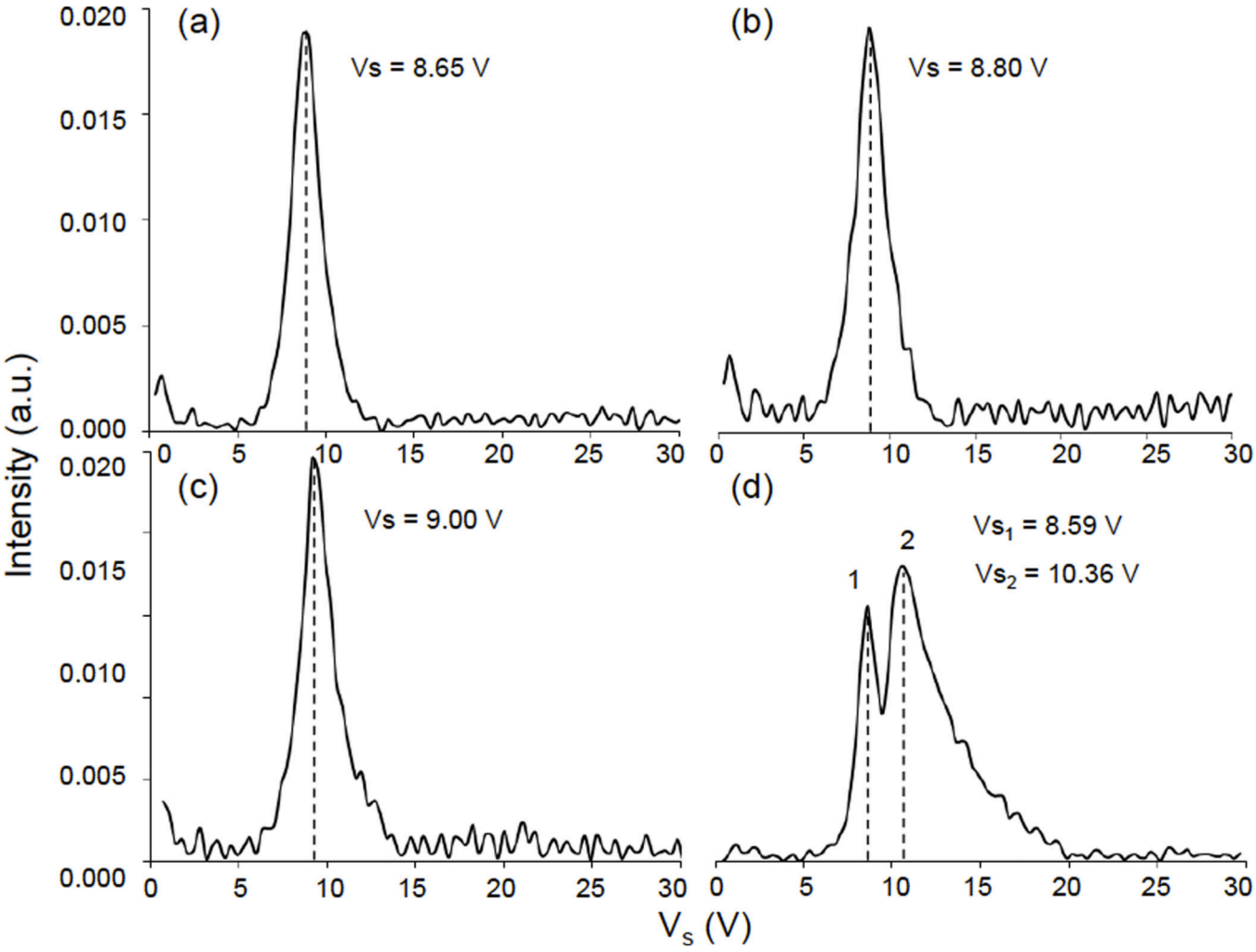

Figure 5:
chemical responses with V_L =3 V and Vs varied from 0 to 30 V for (a) methyl salicylate, (b) naphthalene, (c) benzene, and (d) 2-butanone with benzene as a dopant.

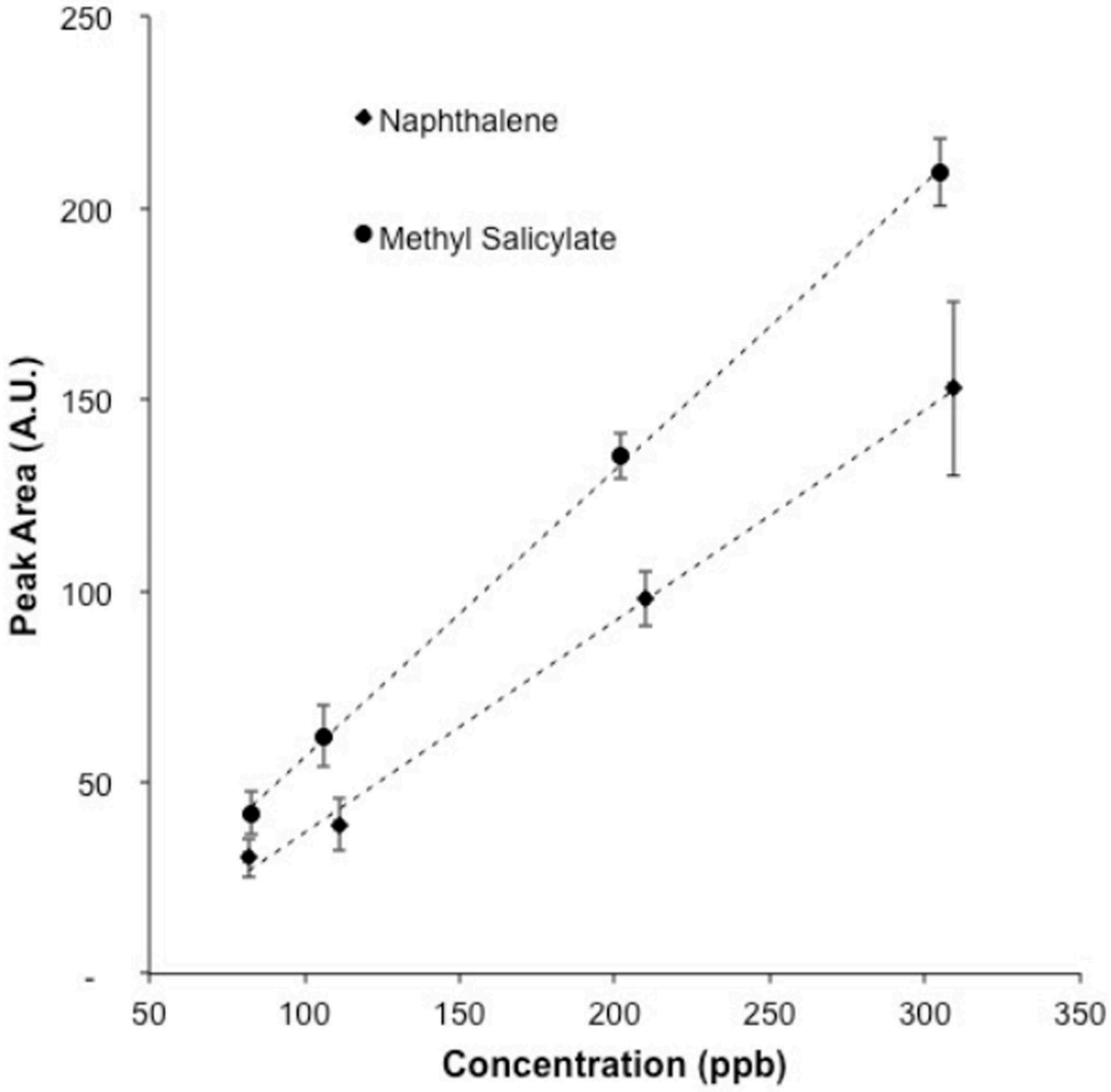

Figure 6:
Calibration curves of naphthalene and methyl salicylate.